Magnetism II [lln23]

The magnetism of transition metals comes from 3d electrons and that of rare earth elements originates in 4f electrons. The latter are more effectively shielded from environmental effects than the former.

Crystal field:

The crystalline environment has a reduced rotational symmetry at the atomic positions. This symmetry depends on the crystal structure.

The five 3d orbitals have distinct shapes with reduced rotational symmetry.

The two orbitals in the group named e_g on the left have more negative charge in the directions of the coordinate axes (x, y, or z) than the three orbitals in the group named t_{2g} on the right.

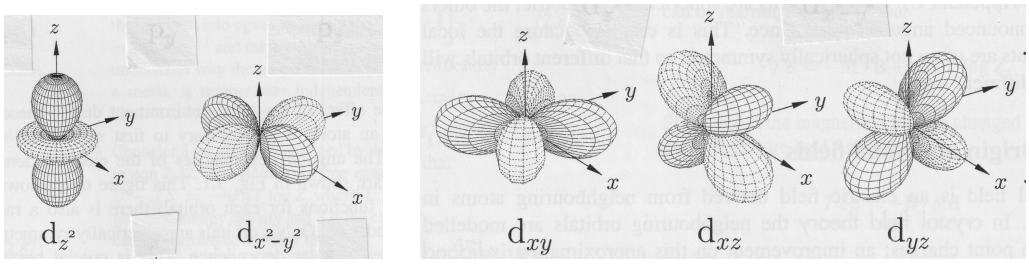

[images from Blundell 2011]

Two common crystalline environments of magnetic ions are octahedral (left) or tetrahedral (right).

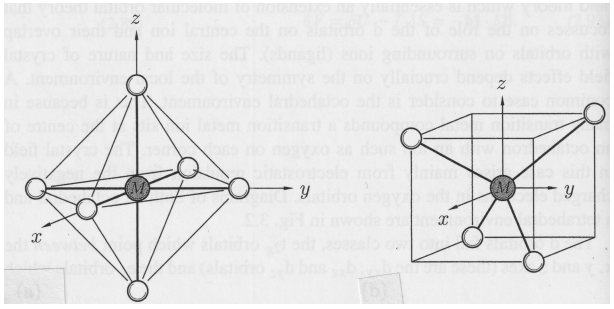

[image from Blundell 2011]

It is evident then that the e_g orbitals have more strongly overlapping wave functions in the octahedral environment than the t_{2g} orbital and vice versa in the tetragonal environment. Overlap causes repulsion.

The result is a crystal field splitting of the 3d energy levels into a group of three and a group of two. The splitting is opposite in the two environments.

Low-field and high-field regimes:

The order in which the levels of the crystal-field split 3d shell are filled by electrons depends on the relative strength of two competing forces:

- crystal field effect (cause of level splitting described above),
- pairing force (Coulomb repulsion of electrons in the same orbital), consistent with Hund's rule #1.

In a *weak-field* environment the pairing force dominates, whereas the crystal field is dominant in a *strong-field* environment.

Example: The Fe^{++} ion has the electron configuration $[Ar]3d^6$ [lln10].

The crystal field is taken to have octahedral symmetry, which places the t_2g triplet below the e_g doublet as shown below.

- ▷ Weak-field environment: single occupancy from the bottom up has priority; the four unpaired electrons produce an effective spin $S = 2$.
- ▷ Strong-field environment: full low-energy level occupancy has priority; the six paired electrons produce an effective spin $S = 0$.

Weak-field (strong-field) environments are often associated with high-spin (low-spin) configurations.

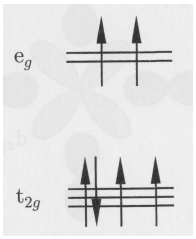

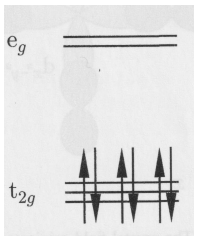

[images from Blundell 2011]

Orbital quenching:

The crystal-field splitting of 3d electrons invalidates Hund's rule #3 [lln22]. The orbital angular momentum is effectively quenched: $\langle \mathbf{L} \rangle = 0$. The magnetic moment is dominated by the resultant spin $\langle \mathbf{S} \rangle$.

It is instructive to compare specifications and Hund's-rule predictions with experimental data for magnetic moments of 3d electrons and 4f electrons.

- ▷ S, L, and J as predicted by Hund's rules.
- ▷ $p = p_1 = \mu/\mu_B = g_J\sqrt{J(J+1)}$ inferred from Hund's rules #1 - #3.
- ▷ $p_2 = \mu/\mu_B = 2\sqrt{S(S+1)}$ inferred from Hund's rule #1.

ion	shell	S	L	J	term	p_1	p_{exp}	p_2
Ti^{3+}, V^{4+}	$3d^1$	$\frac{1}{2}$	2	$\frac{3}{2}$	$^2D_{3/2}$	1.55	1.70	1.73
V^{3+}	$3d^2$	1	3	2	$^3F_2$	1.63	2.61	2.83
Cr^{3+}, V^{2+}	$3d^3$	$\frac{3}{2}$	3	$\frac{3}{2}$	$^4F_{3/2}$	0.77	3.85	3.87
Mn^{3+}, Cr^{2+}	$3d^4$	2	2	0	$^5D_0$	0	4.82	4.90
Fe^{3+}, Mn^{2+}	$3d^5$	$\frac{5}{2}$	0	$\frac{5}{2}$	$^6S_{5/2}$	5.92	5.82	5.92
Fe^{2+}	$3d^6$	2	2	4	$^5D_4$	6.70	5.36	4.90
Co^{2+}	$3d^7$	$\frac{3}{2}$	3	$\frac{9}{2}$	$^4F_{9/2}$	6.63	4.90	3.87
Ni^{2+}	$3d^8$	1	3	4	$^3F_4$	5.59	3.12	2.83
Cu^{2+}	$3d^9$	$\frac{1}{2}$	2	$\frac{5}{2}$	$^2D_{5/2}$	3.55	1.83	1.73
Zn^{2+}	$3d^{10}$	0	0	0	$^1S_0$	0	0	0

ion	shell	S	L	J	term	p	p_{exp}
Ce^{3+}	$4f^1$	$\frac{1}{2}$	3	$\frac{5}{2}$	$^2F_{5/2}$	2.54	2.51
Pr^{3+}	$4f^2$	1	5	4	$^3H_4$	3.58	3.56
Nd^{3+}	$4f^3$	$\frac{3}{2}$	6	$\frac{9}{2}$	$^4I_{9/2}$	3.62	3.3–3.7
Pm^{3+}	$4f^4$	2	6	4	$^5I_4$	2.68	–
Sm^{3+}	$4f^5$	$\frac{5}{2}$	5	$\frac{5}{2}$	$^6I_{5/2}$	0.85	1.74
Eu^{3+}	$4f^6$	3	3	0	$^7F_0$	0.0	3.4
Gd^{3+}	$4f^7$	$\frac{7}{2}$	0	$\frac{7}{2}$	$^8S_{7/2}$	7.94	7.98
Tb^{3+}	$4f^8$	3	3	6	$^7F_6$	9.72	9.77
Dy^{3+}	$4f^9$	$\frac{5}{2}$	5	$\frac{15}{2}$	$^6H_{15/2}$	10.63	10.63
Ho^{3+}	$4f^{10}$	2	6	8	$^5I_8$	10.60	10.4
Er^{3+}	$4f^{11}$	$\frac{3}{2}$	6	$\frac{15}{2}$	$^4I_{15/2}$	9.59	9.5
Tm^{3+}	$4f^{12}$	1	5	6	$^3H_6$	7.57	7.61
Yb^{3+}	$4f^{13}$	$\frac{1}{2}$	3	$\frac{7}{2}$	$^2F_{7/2}$	4.53	4.5
Lu^{3+}	$4f^{14}$	0	0	0	$^1S_0$	0	0

[images from Blundell 2011]

Quenching is largely absent in the case of 4f electrons, which are well shielded from crystal-field effects. Quenching for 3d electrons increases the predictive power of Hund's rule #1.

The quenching is neither complete nor absent in transition elements with incomplete 4d and 5d shells (not shown).

Jahn-Teller effect:

The atomic level spectrum does not passively adjust to the crystal-field environment. In some cases, the electrons "strike back" quite noticeably.

The Jahn-Teller effect in its simplest realization describes a spontaneous lattice distortion combined with a splitting of degenerate levels at and near the bottom of the spectrum.

Example: The Mn^{3+} ion has the electron configuration [Ar]$3d^4$ [lln10].

In a weak-field octahedral crystal field environment, the four 3d electrons prefer single occupancy from the bottom up as shown on the left.

A tetragonal distortion of the octahedral crystal-field environment is uniaxial. Here it elongates the distances in z-direction and compresses them in the x and y direction.

Quite generally, a lowering of the environmental symmetry causes a splitting of some if not all degenerate atomic levels. The effect in this example is shown going from left to right.

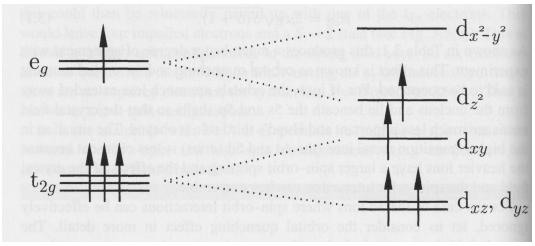

[image from Blundell 2011]

The lattice distortion can be quantified by some parameter Q, which grows continuously from zero at the point of higher (octahedral) symmetry.

The lattice distortion costs elastic energy that grows quadratically in Q. The level splittings, on the other hand, tend to grow linearly in Q.

In the example shown, the net energy of the four occupied levels descends linearly in Q, e.g. $-aQ$, as the elastic energy grows like $+bQ^2$. The lowest-energy state is realized for $Q_0 = a/2b$, with lower (tetragonal) symmetry.

This is an instance of interaction-mediated symmetry breaking. All forces in action are consistent with the higher (octahedral) symmetry. Yet they spontaneously produce a state of lower (tetragonal) symmetry.

Notice the absence of a clear-cut cause-and-effect relation, which is typical for interactions.

Nuclear magnetic resonance:

The experimental probe named *Nuclear Magnetic Resonance* (NMR) has its most well-known application in *Magnetic Resonance Imaging* (MRI).

NMR probes the magnetic environment at positions of atomic nuclei with non-vanishing nuclear spin I, e.g. ^{1}H ($I = \frac{1}{2}$), ^{2}H ($I = 1$), or ^{13}C ($I = \frac{1}{2}$).

Nuclear spins tend to be well shielded from strong interactions with other degrees of freedom. A strong external magnetic field $\mathbf{B}_0$ is then easily the dominant interaction:

$$\mathcal{H}_0 = -\boldsymbol{\mu} \cdot \mathbf{B}_0, \quad \boldsymbol{\mu} = g_I \mu_{\rm N} \mathbf{I}.$$

It is safe to assume that the nuclear spin I in question stays in the ground state and that the relevant energy level spectrum is

$$E = -g_I \mu_{\rm N} B_0 m_I, \quad m_I = -I, -I+1, \ldots, +I.$$

Adjacent levels, i.e. levels with $\Delta m_I = \pm 1$, resonate with electromagnetic radiation at frequency ω, where $\hbar\omega = \Delta E = g_I \mu_{\rm N} B_0$. Photons have spin $s = 1$, which is consistent with the selection rule $\Delta m_I = \pm 1$.

NMR spectrometers which use magnetic fields around 10T or higher produce resonance frequencies in the radio frequency (RF) range, amounting to tens or hundreds of MHz.

For the discussion that follows we focus on a two-level system, i.e. on a physical ensemble of nuclear spins $I = \frac{1}{2}$. At thermal equilibrium the populations N_+ and N_- of the upper and lower levels, respectively, have the ratio,

$$\left(\frac{N_+}{N_-}\right)_{\rm eq} = e^{-\beta\hbar\omega}.$$

This ratio can be driven toward unity by radiation at the resonant frequency, which induces processes of absorption and stimulated emission. We can write,

$$\frac{d}{dt} N_+(t) = W[N_-(t) - N_+(t)], \quad \frac{d}{dt} N_-(t) = W[N_+(t) - N_-(t)].$$

The transition rate W is proportional to the intensity of the radiation.

In the absence of spontaneous emission or emission stimulated by interactions with other degrees of freedom, the difference in level populations approaches zero exponentially at a rate dictated by the intensity of the radiation:

$$n(t) \doteq N_-(t) - N_+(t) \quad \Rightarrow \; \frac{d}{dt} n(t) = -2W n(t)$$
$$\Rightarrow \; n(t) = n_{\rm eq} e^{-2Wt}, \quad n_{\rm eq} = N_-^{(\rm eq)} \left[1 - e^{-\beta\hbar\omega}\right].$$

Counteracting this process of population equalization are processes caused by interactions with electronic degrees of freedom, which depopulate the upper level relative to the lower level.

These interactions are, for the most part, environmental effects associated with the location of the atomic nucleus in a crystal lattice. Their effect is summarily accounted for in what is named *spin-lattice relaxation time* T_1.

Spin-lattice relaxation processes restore the equalized level populations to their equilibrium values on the time scale of T_1 once irradiation has ceased:

$$n(t) = n_{\mathrm{eq}}\big[1 - e^{-t/T_1}\big].$$

If irradiation is initiated in the face of spin-lattice relaxation processes, then the level equalization remains incomplete. In the (linear) ODE,

$$\frac{d}{dt}n(t) = -2Wn(t) + \frac{n_{\mathrm{eq}} - n(t)}{T_1},$$

the first term on the right-hand side is due to irradiation and the second term due to spin-lattice relaxation. The exact solution for two different initial condition [lex171],

$$n(t) = \frac{n_{\mathrm{eq}}}{1 + 2T_1W}\left[1 - e^{-(t/T_1)(1+2T_1W)}\right] \quad : \; n(0) = 0,$$
$$n(t) = \frac{n_{\mathrm{eq}}}{1 + 2T_1W}\left[1 + 2T_1We^{-(t/T_1)(1+2T_1W)}\right] \quad : \; n(0) = n_{\mathrm{eq}},$$

depends on two characteristic times, $1/W$ and T_1, the former associated with the depopulation of the lower level and the latter with its repopulation.

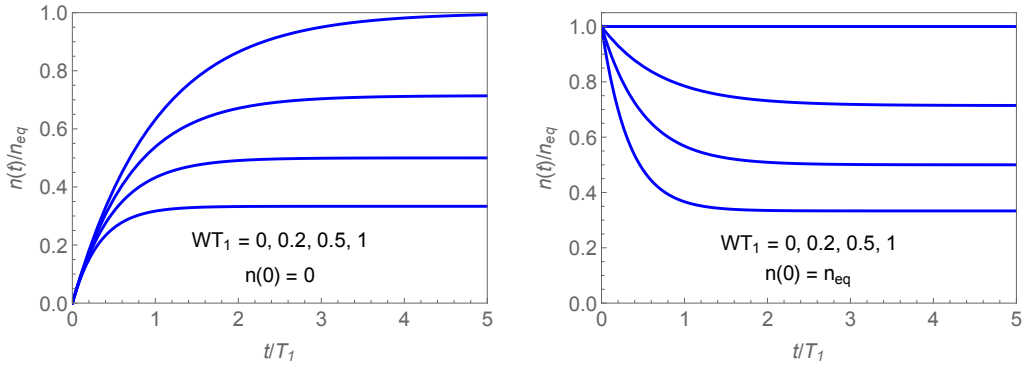

The stationary lower-level excess population is increasingly suppressed from the equilibrium value as the radiation intensity increases ($\propto W$):

$$\lim_{t\to\infty} n(t) = \frac{n_{\mathrm{eq}}}{1 + 2T_1W}.$$

The rate at which energy is absorbed by the nuclear spin during irradiation and spin-lattice relaxation is [lex171]:

$$\frac{dE}{dt}\Big|_{\text{abs}} = \hbar\omega W n(t) \;\stackrel{t\to\infty}{\longrightarrow}\; \hbar\omega n_{\text{eq}} \frac{W}{1+2T_1W}.$$

At low radiation intensity, this rate grows like $n_{\text{eq}}\hbar\omega W$. Here it is governed by the time scale $1/W$. At higher intensity it saturates at $n_{\text{eq}}\hbar\omega/2T_1$, where it is governed by the time scale T_1.

Bloch equations:

In the following we treat nuclear magnetism as a physical ensemble of classical magnetic moments interacting primarily with an external magnetic field $\mathbf{B}$. The equation of motion for the net magnetization reads,

$$\frac{d}{dt}\mathbf{M} = \gamma \mathbf{M} \times \mathbf{B}.$$

A solution for a constant and uniform field $\mathbf{B} = B_z\,\hat{\mathbf{k}}$ describes a vector $\mathbf{M}$ of constant length precessing uniformly about the z-axis:

$$\frac{dM_x}{dt} = \gamma M_y B_z, \quad \frac{dM_y}{dt} = -\gamma M_x B_z, \quad \frac{dM_z}{dt} = 0,$$

$$\Rightarrow\; M_z = \text{const}, \quad M_x = M_\perp \sin(\omega t), \quad M_y = M_\perp \cos(\omega t), \quad \omega = \gamma B_z.$$

The constant nonzero M_z can be interpreted as representing the stationary result $n_{\text{eq}} > 0$ of the two-level system considered earlier, where stationarity is reached on the time scale of T_1 (*spin-lattice relaxation time*).

The rotating $\mathbf{M}_\perp = M_x\,\hat{\mathbf{i}} + M_y\,\hat{\mathbf{j}}$ is known experimentally to relax to zero on a faster time scale T_2 (*spin-spin relaxation time*), caused by a process of dephasing. Different spins experience (owing to diverse causes) slightly different magnetic fields B_z, which modifies the precession frequencies ω.

The equations of motion amended to account for both spin-lattice and spin-spin relaxation are named *Bloch equations* [lex174][lex175]:

$$\begin{aligned}
\frac{dM_x}{dt} &= \gamma[M_y B_z - M_z B_y] - \frac{M_x}{T_2}, \\
\frac{dM_y}{dt} &= \gamma[M_z B_x - M_x B_z] - \frac{M_y}{T_2}, \\
\frac{dM_z}{dt} &= \gamma[M_x B_y - M_y B_x] + \frac{M_{\text{eq}} - M_z}{T_1}.
\end{aligned}$$

A nonzero $\mathbf{M}_\perp$, which then rotates and dephases, can be produced from the equilibrium state with $M_z > 0$, $M_x = M_y = 0$ by ashort pulse of magnetic field B_y, for example, causing a 90° rotation of M_z toward the xy-plane.

Electron spin resonance:

Electron Spin Resonance (ESR), also named *Electron Paramagnetic Resonance* (EPR) is analogous to NMR in many respects.

The electron magnetic moment is much larger than nuclear magnetic moments, implying that the resonance frequencies are typically much higher. Experiments use microwave cavities and tune external magnetic fields.

Microwave frequencies (GHz) are ideally suited for the investigation of crystal-field effects on atomic spectra. A complication in the analysis of ESR data is the hyperfine splitting of degenerate levels.

One notable example is the magnetic-field splitting of the Kramers doublet in the cerium ion Ce^{3+}, whose electronic structure is [Xe]4f.

The lone 4f electron has $L = 3$ and $S = \frac{1}{2}$. Spin-orbit coupling and Hund's rule predict a ground state with $J = \frac{5}{2}$, which hase sixfold degeneracy.

The axial crystal field splits this multiplet into three doublets. The lowest doublet with $m_J = \pm\frac{1}{2}$ is a *Kramers doublet*.

Such ground-state degeneracies for ions with an odd number of electrons were predicted by Kramers on general grounds using time reversal symmetry.

A magnetic-field splitting of this Kramers doublet up to ~ 0.1meV is manageable with typical lab equipment. This puts into the ESR detection range.

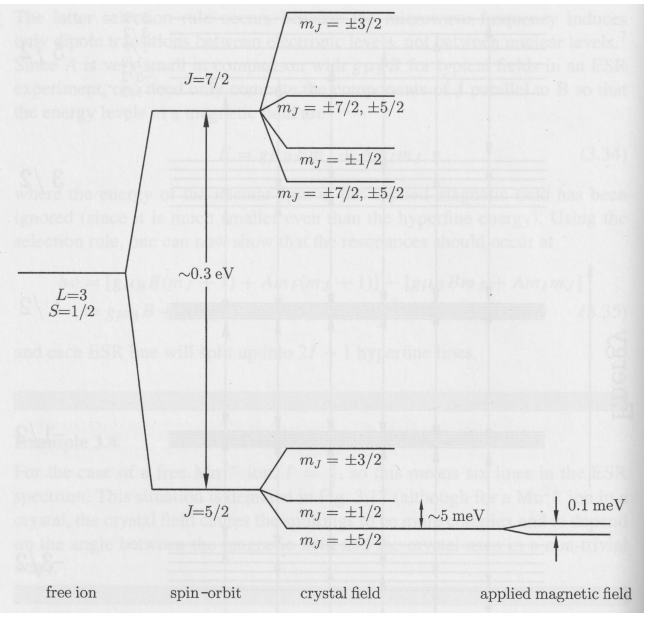

[image from Blundell 2011]

Mössbauer spectroscopy:

Photons emitted from or absorbed by an atom produce recoil motion. In [lex94] we investigated this effect using energy and momentum conservation. The effect holds for photons associated with electronic or nuclear transitions.

Transitions with long radiative lifetimes have small linewidth [lln24]. A (radioactive) source of ^{57}Co nuclei emits, in the wake of its β-decay into ^{57}Fe, 14.4keV photons in a slow transition to the ground state.

In the case of free atoms the resonance conditions for emission and absorption are significantly different for this transition. Emission photons have not nearly enough energy to become absorption photons.

However, if the source (^{57}Co nuclei) and the target (^{57}Fe in the ground state) are bound into the lattice of a solid material, both emission and absorption are essentially without recoil. The momentum is carried by the entire crystal.

The (extremely sharp) emission and absorption lines of the same transition are then very close together. The highly precarious resonance condition can be tuned via motion of the source relative to the target (Doppler effect).

Mössbauer spectroscopy is famous for its high sensitivity. The smallest environmental effects on the energy levels of the target nucleus are detectible or the smallest changes in relative velocity between source and target.

Muon-spin rotation:

The protagonist of the muon-spin rotation (μSR) probe is the positively charged lepton μ^+ as produced in the lab from pion decay: $\pi^+ \to \mu^+ + \nu_\mu$.

The neutrino is left-handed, meaning that its spin is antiparallel to its momentum. If the (spinless) π^+ decays while at rest, the μ^+ has its spin also directed opposite to its momentum.

A beam of μ^+ particles thus produced is slowed close to rest by charge interaction processes, which have no effect on the μ^+ spin polarization. The μ^+ is attracted to electrons and may form hydrogen-like muonium.

The spin of the implanted μ^+ is highly sensitive to local magnetic fields. It undergoeas Larmor precession at angular frequency $\omega = \gamma_\mu B$.

In a μSR experiment, what is detected is not the μ^+ but the positron emerging from its decay: $\mu^+ \to e^+ + \nu_\mathrm{e} + \bar{\nu}_\mu$. This parity violating process emits e^+ particles with an enhanced probability in the direction of the muon spin. The positron beams thus rotates in sync with the precessing muon spin.

Exchange interaction:

As a backdrop to what follows, we recall from [lln12] and [lln13] the *magnetic dipole interaction* between magnetic moments $\boldsymbol{\mu}_1$ and $\boldsymbol{\mu}_2$ such as those associated with magnetic atoms a distance r apart:

$$U = \frac{\mu_0}{4\pi r^3}\big[\boldsymbol{\mu}_1 \cdot \boldsymbol{\mu}_2 - 3(\boldsymbol{\mu}_1 \cdot \hat{\mathbf{r}})(\boldsymbol{\mu}_2 \cdot \hat{\mathbf{r}})\big], \quad \hat{\mathbf{r}} \doteq \frac{\mathbf{r}}{r}.$$

The strength of this interaction, estimated by the Bohr magneton and a very short interatomic distance, $(\mu_0/4\pi)\mu_{\mathrm{B}}^2/(1\text{Å})^3 \sim 10^{-23}$J, yields an energy equal to that of thermal fluctuations at temperatures ~ 1K.

The magnetic dipole interaction is far too weak to qualify as an agent of magnetic ordering at room temperature or higher. Finding the right agent had to await the advent of quantum mechanics.

The *exchange interaction*, much stronger than the magnetic dipole interaction and of shorter range, has its foundation in Coulomb repulsion and symmetry principles of quantum statistics.

For a simple demonstration, consider two electrons in atomic orbitals a, b. Electrons have spin $\frac{1}{2}$, hence they are fermions. The two-particle wave function must be antisymmetric under permutation (exchange of location).

Recalling the explanations given in [lln22] about the spatial and spin parts of the two-electron wave function, we write

$$\Psi_{\mathrm{S}}(\mathbf{r}_1, \mathbf{r}_2) = \frac{1}{\sqrt{2}}\Big[\phi_a(\mathbf{r}_1)\phi_b(\mathbf{r}_2) + \phi_a(\mathbf{r}_2)\phi_b(\mathbf{r}_1)\Big]\chi_{\mathrm{S}},$$
$$\Psi_{\mathrm{T}}(\mathbf{r}_1, \mathbf{r}_2) = \frac{1}{\sqrt{2}}\Big[\phi_a(\mathbf{r}_1)\phi_b(\mathbf{r}_2) - \phi_a(\mathbf{r}_2)\phi_b(\mathbf{r}_1)\Big]\chi_{\mathrm{T}},$$

where S stands for spin singlet ($s = 0$) and T for spin triplet ($s = 1$). Ψ_{S} has a symmetric spatial part and an antisymmetric spin part, while the opposite is the case for Ψ_{T}. Both wave functions are antisymmetric overall.

The interaction Hamiltonian $\mathcal{H}$ contains kinetic energy and Coulomb repulsion but no significant interaction between electron spins. The energies of the singlet and triplet states in first-order perturbation theory become,

$$E_{\mathrm{S}} = \int d\mathbf{r}_1 d\mathbf{r}_2 \Psi_{\mathrm{S}}^*(\mathbf{r}_1, \mathbf{r}_2)\mathcal{H}\Psi_{\mathrm{S}}(\mathbf{r}_1, \mathbf{r}_2), \quad E_{\mathrm{T}} = \int d\mathbf{r}_1 d\mathbf{r}_2 \Psi_{\mathrm{T}}^*(\mathbf{r}_1, \mathbf{r}_2)\mathcal{H}\Psi_{\mathrm{T}}(\mathbf{r}_1, \mathbf{r}_2).$$

The level spacing between singlet and triplet states is determined by the *exchange integral* [lex176],

$$E_{\mathrm{S}} - E_{\mathrm{T}} = 2\int d\mathbf{r}_1 d\mathbf{r}_2 \phi_a^*(\mathbf{r}_1)\phi_b^*(\mathbf{r}_2)\mathcal{H}\phi_a(\mathbf{r}_2)\phi_b(\mathbf{r}_1) \doteq 2J,$$

governed entirely by the charge distribution of the two electrons.

The mere fact that $\Psi_{\rm S}$ and $\Psi_{\rm T}$ have not only different spatial parts but also different spin parts makes it possible to express the level spacing $2J$ as an effective interaction between electron spins.

Applying the operator identity for two spins s,

$$(\mathbf{S}_1 + \mathbf{S}_2)^2 = (\mathbf{S}_1)^2 + (\mathbf{S}_2)^2 + 2\mathbf{S}_1 \cdot \mathbf{S}_2,$$

two the case $s = \frac{1}{2}$ we obtain,

$$\left.\begin{array}{c} 2 \\ 0 \end{array}\right\} = \frac{3}{4} + \frac{3}{4} + 2\mathbf{S}_1 \cdot \mathbf{S}_2 \quad \Rightarrow \; \mathbf{S}_1 \cdot \mathbf{S}_2 = \left\{\begin{array}{c} \frac{1}{4}\ (\mathrm{T}) \\ -\frac{3}{4}\ (\mathrm{S}) \end{array}\right. .$$

If we construct the replacement Hamiltonian in the form,

$$\mathcal{H}_{\rm ex} \doteq \frac{1}{4}\underbrace{(E_{\rm S} + 3E_{\rm T})}_{\rm const} - \underbrace{(E_{\rm S} - E_{\rm T})}_{2J}\mathbf{S}_1 \cdot \mathbf{S}_2,$$

we can recover the same two energy levels by an operator now acting on the spin part of the two-electron wave function:

$$\int d\mathbf{r}_1 d\mathbf{r}_2 \Psi_T^* \mathcal{H}_{\rm ex} \Psi_{\rm T} = \langle \chi_{\rm T} | \mathcal{H}_{\rm ex} | \chi_{\rm T} \rangle = \frac{1}{4}(E_{\rm S} + 3E_{\rm T}) - \frac{1}{4}(E_{\rm S} - E_{\rm T}) = E_{\rm T},$$
$$\int d\mathbf{r}_1 d\mathbf{r}_2 \Psi_S^* \mathcal{H}_{\rm ex} \Psi_{\rm S} = \langle \chi_{\rm S} | \mathcal{H}_{\rm ex} | \chi_{\rm S} \rangle = \frac{1}{4}(E_{\rm S} + 3E_{\rm T}) + \frac{3}{4}(E_{\rm S} - E_{\rm T}) = E_{\rm S}.$$

Depending on circumstances, the exchange integral can be positive (favoring spin alignment) or negative (favoring anti-alignment).

- Realizations of $J > 0$ are common for electrons sharing incomplete shells of the same atom, in accordance with Hund's rule #1. The spatial wave function is antisymmetric, which separates the charges of the two electrons more effectively. The spin triplet has lower energy.
- Realizations of $J < 0$ are common for unpaired electrons on neighboring atoms. The spatial wave function of the spin singlet is symmetric, which allows more (negative) electronic charge to be located between the (positive) nuclear charges, thus lowering Coulomb repulsion.

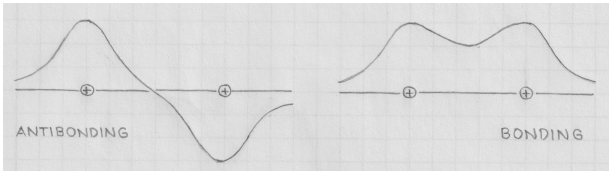

The exchange integral can be a significant factor in molecular bonding.

The kinetic energy is also a factor of significance in bonding. Its magnitude locally is indicated by the curvature of the wave function (2^{nd} derivative). Tight confinement enhances curvature. Bonding loosens confinement.

The need for wave-function overlap makes the exchange interaction short-ranged, in contrast to the (much weaker) dipole interaction.

The exchange interaction in magnetic insulators is typically represented by a model Hamiltonian of the form,

$$\mathcal{H} = -\sum_{i,j} J_{ij} \mathbf{S}_i \cdot \mathbf{S}_j,$$

for statistical mechanical analysis. The double sum is over the sites of lattice. The exchange constant for all pairs i, j except nearest-neighbor sites are often negligibly small.

$J_{ij} > 0$, which favors spin alignment, is the cause of ferromagnetic ordering. Anti-alignment is favored if $J_{ij} < 0$. On a bipartite lattice, preferred anti-alignment of nearest-neighbor spins leads to antiferromagnetic ordering.

Mediated exchange interaction:

We know from earlier that paramagnetism is prevalent in ions with partially filled d or f shells, neither of which is outermost. Direct wave-function overlap tends to be weak for unpaired d or f electrons in insulating materials, hence ineffective as agents of direct exchange interaction.

Here we briefly describe three types of mediated exchange interaction.

- *Superexchange*: Exchange interaction in magnetic insulators can be mediated by non-magnetic ions, e.g. by non-magnetic O^{2-} ions between the sites of magnetic Mn^{2+} ions in the compound MnO, producing antiferromagnetism in this case.

  The strength and the sign of the effective exchange constant J mediated by the superexchange mechanism varies with bond angle. This provides a powerful design tool to magneto-chemists.

- *Itinerant exchange*: In metals the exchange interaction can be mediated by conduction electrons, a topic to be discussed in a later module. Itinerant exchange has a longer range,

  $$J_{\text{RKKY}} \propto \frac{\cos(k_{\text{F}} r)}{r^3},$$

  where $\hbar k_F$ is the Fermi momentum of the partially filled band of magnetically relevant electrons.

– *Double exchange*: One form of indirect exchange is mediated by electron hopping in mixed-valency magnetic materials. In $La_{1-x}Sr_xMnO_3$ (Sr doped $LaMnO_3$), Lanthanum is present as trivalent La^{3+} and Strontium as (divalent) Sr^{2+}.

This compound contains two types of magnetic ions: a fraction x of Mn^{4+} with three 3d electrons and a fraction $1-x$ of Mn^{3+} with four 3d electrons.

Recall the splitting of the five 3d orbitals into two groups e_g and t_{2g} discussed earlier. Hund's rule favors alignment of the three or four 3d electrons.

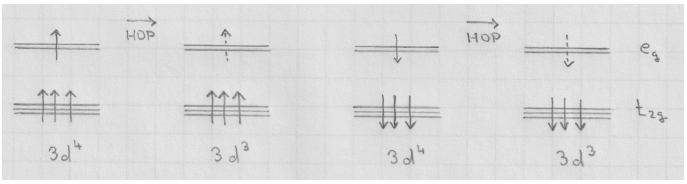

The compound $LaMnO_3$ has the (upper) e_g group of levels singly occupied at all Mn sites. The material is insulating and antiferromagnetic. The superexchange coupling between the Mn ions is mediated by oxygen.

Doping removes the 3d electron in the e_g group on a fraction x of Mn sites. Hopping of the e_g electron between Mn ions is a mechanism that lowers the average kinetic energy due to the more relaxed confinement of that electron.

Hopping takes place without spin-flip (a key fact). It only takes place between if the electrons in the t_{2g} are aligned on both sites. *Intra-ion exchange* coupling (Hund's rule) makes hopping costly otherwise.

Ferromagnetic alignment of all 3d electrons facilitates hopping, which is associated with an energetic incentive. Hopping thus mediates a form of *inter-ion exchange* coupling. Hence the name double exchange.

Hopping increases the conductivity by orders of magnitude. The doped compound becomes metallic.